0026-895X/98/020283-12$3.00/0

MOLECULAR PHARMACOLOGY, **53:**283–294 (1998).

Ivermectin: A Positive Allosteric Effector of the α7 Neuronal Nicotinic Acetylcholine Receptor

RYOKO M. KRAUSE, BRUNO BUISSON, SONIA BERTRAND, PIERRE-JEAN CORRINGER, JEAN-LUC GALZI,[1] JEAN-PIERRE CHANGEUX, and DANIEL BERTRAND

Department of Physiology, University Medical Center, 1211 Geneva 4, Switzerland (R.M.K., B.B., S.B., D.B.), and URA Centre National de la Recherche Scientifique D1284, Neurobiologie Moléculaire, Institut Pasteur, 75724 Paris Cedex 15, France (P.-J.C., J.-L.G., J.-P.C.)

Received June 26, 1997; Accepted October 14, 1997

This paper is available online at http://www.molpharm.org

ABSTRACT

We report that preapplication of ivermectin, in the micromolar range, strongly enhances the subsequent acetylcholine-evoked current of the neuronal chick or human α7 nicotinic acetylcholine receptors reconstituted in *Xenopus laevis* oocytes and K-28 cells. This potentiation does not result from nonspecific Cl^- currents. The concomitant increase in apparent affinity and cooperativity of the dose-response curve suggest that ivermectin acts as a positive allosteric effector. This interpretation is supported by the observation of an increase in efficiency of a partial agonist associated with the potentiation and by the differential effect of ivermectin on mutants within the M2 channel domain. Ivermectin effects reveal a novel allosteric site for pharmacological agents on neuronal α7 nicotinic acetylcholine receptors.

Nicotine, the pharmacologically active compound of tobacco leaves, mimics several characteristic effects of the natural ligand ACh in the nervous system through the activation of ACh-gated ion channels, referred as nicotinic. nAChRs belong to the superfamily of ligand-gated channels and have been shown to share a number of structural and functional homologies with other members, such as $GABA_A$, glycine, and serotoninergic receptors (Bertrand and Changeux, 1995; Lindstrom, 1996). It is thought that like the muscle nAChR, a single neuronal receptor results from the assembly of five subunits, each of which spans the membrane four times. Although only five genes are known to code for the two muscle nAChRs, 11 subunits have been identified for the neuronal nAChRs [α2–9, β2, β3, and β4 (for a review, see Lindstrom, 1996)]. Homomers or different combinations of these neuronal nAChR subunits have been shown to be expressed in the peripheral and central nervous systems (Bertrand and Changeux, 1995). Based on the alignment of their protein sequences and physiological as well as pharmacological properties, these subunits can be subdivided further into two main groups: those that contribute to receptors that are sensitive to the snake toxin αBgt and those that do not bind this toxin. Another important distinction is that the three αBgt-sensitive subunits (α7–9) can reconstitute functional homomeric receptors when expressed in a host system. The α7 subunit is expressed strongly in the brain, and a high degree of correlation is observed between αBgt labeling and *in situ* hybridization with α7 mRNA probes (Wevers *et al.*, 1995).

Among the homomeric nAChRs, the α7 subunit is by far the most studied, and it frequently is used as a model of the nAChR family (for a review, see Bertrand and Changeux, 1995). Physiological characterizations showed that the receptor reconstituted with this subunit is highly permeable to Ca^{2+} with a selectivity pCa/pNa ratio of $\geq$10:1 (Bertrand *et al.*, 1993). It later was shown that the influx of Ca^{2+} observed during receptor activation by ACh is sufficient to trigger an increase in the intracellular Ca^{2+} concentration (Delbono *et al.*, 1997). In addition, it was shown that activation by low nicotine concentration of an αBgt-sensitive subunit in rat hippocampal cultured neurons results in an increase in the release of the glutamate neurotransmitter (Gray *et al.*, 1996). Similarly, nicotinic agonist enhanced the release of the neurotransmitter GABA in the mouse thalamus (Léna and Changeux, 1997).

An important feature of the neuronal nAChRs is the neg-

This work was supported by the Swiss National Foundation and the Office Fédéral de l'Education et des Sciences (D.B.) and Collège de France, Association Française contre la Myopathie, Institut de la Santé et de la Recherche Médicale, Direction de la Recherche Etudes et Techniques, and Commission of the European Communities (Biotech, Biomed) (J.P.C.).

[1] Current affiliation: Centre National de la Recherche Scientifique, 67400 Illkirch, France.

ABBREVIATIONS: ACh, acetylcholine; nAChR, nicotinic acetylcholine receptor; GABA, γ-aminobutyric acid; $GABA_AR$, γ-aminobutyric acid receptor; HEPES, 4-(2-hydroxyethyl)-1-piperazineethanesulfonic acid; IVM-PO_4, 22,23-dihydroavermectin $B1_a$ 4″-*O*-phosphate; BAPTA, 1,2-bis(2-aminophenoxy)ethane-*N*,*N*,*N*′,*N*′-tetraacetic acid; I-V, current/voltage; DMPP, 1,1-dimethyl-4-phenylpiperazinium; MLA, methyllycaconitine; IVM, ivermectin.

ative or positive allosteric regulations caused by a variety of pharmacological agents (Bertrand *et al.*, 1991b; Mulle *et al.*, 1992; Valera *et al.*, 1992; Galzi *et al.*, 1996a; Buisson and Bertrand, 1998). For example, steroids have been found to inhibit neuronal nAChRs through allosteric interactions (Valera *et al.*, 1992). This property is shared by both the heteromeric and homomeric receptors, as recently shown with the human $\alpha4\beta2$ and $\alpha7$ nAChRs (Buisson and Bertrand, 1998). On the contrary, it was shown that neuronal nAChRs are potentiated strongly by the extracellular Ca^{2+} concentration (Mulle *et al.*, 1992; Galzi *et al.*, 1996d). The combination of site-directed mutagenesis with electrophysiology recently led to the identification of a Ca^{2+} binding site in the extracellular domain of the $\alpha7$ subunit (Galzi *et al.*, 1996a).

The specific loss of nAChR binding sites observed in the brain of patients with neurodegenerative diseases such as Alzheimer's or Parkinson's suggests that these receptors may play a critical role in the evolution of these disorders (Warpman and Nordberg, 1995). Furthermore, stimulation of nAChRs in affected patients either by selective agonists or by compounds reducing the activity of acetylcholinesterase shows positive effects on the patients' overall cognitive abilities. A complementary approach would be to use positive allosteric effectors that could selectively enhance the activity of neuronal nAChRs.

Although many compounds have been shown to behave as positive allosteric modulators on the $GABA_AR$ (for a review, see Rabow *et al.*, 1995), much less is known about the neuronal nAChRs. The recent demonstration that the well known anthelmint IVM is a powerful allosteric modulator of worm glutamate receptors (Cully *et al.*, 1994) and that these cloned subunits share homologies with the nAChRs prompted us to examine the effect of this compound on neuronal nAChRs.

In the current work, we studied the effects of IVM on chick and human homomeric $\alpha7$ nAChRs reconstituted in *Xenopus laevis* oocytes and in K-28 cells. We found that although IVM alone induces no detectable current, preapplications of IVM strongly enhance successive ACh-evoked currents. Investigation of the mechanisms underlying IVM potentiation suggests that this compound acts directly on the receptor protein as a positive allosteric effector.

Materials and Methods

Oocyte preparation and cDNA injection. *X. laevis* oocytes were isolated and prepared as described previously (Bertrand *et al.*, 1991a). The oocytes were injected intranuclearly with 2 ng of expression vector cDNA and maintained at 18° in Barth's medium (88 mM NaCl, 1 mM KCl, 2.4 mM $NaHCO_3$, 10 mM HEPES, 0.82 mM $MgSO_4{\cdot}7H_2O$, 0.33 mM $Ca(NO_3)_2{\cdot}4H_2O$, 0.41 mM $CaCl_2{\cdot}6H_2O$, pH 7.4 adjusted with NaOH) with antibiotics (20 μg/ml kanamycin, 100 units/ml penicillin, and 100 μg/ml streptomycin). To improve cell survival and minimize possible contamination, each oocyte was placed in one of the 96-well microtiter plates (Nunc, Naperville, CT).

Drugs and solutions. Drugs and chemicals were purchased from Sigma Chemical (St. Louis, MO) or Fluka Chemical (Ronkonkoma, NY). The IVM used in all the experiments was an essentially pure (>98%) form of 22,23-dihydroavermectin B1a. IVM and IVM-PO_4 were kindly provided by Drs. J. M. Schaeffer and A. Etter (Merck Research Labs, West Point, PA). IVM was dissolved in dimethylsulfoxide. Application of the vehicle alone induced no significant modification of the ACh-evoked currents. To minimize the possible contamination of endogenous Ca^{2+}-activated Cl^- current, OR2-Ba^{2+} was used in most experiments as a bath solution (82.5 mM NaCl, 2.5 mM KCl, 5 mM HEPES, 2.5 mM $BaCl_2$, 1 mM $MgCl_2$, pH 7.4 adjusted with NaOH). All recording solutions were supplemented with 0.5 μM atropine to block possible endogenous muscarinic responses.

Mutagenesis. The chick $\alpha7$ cDNA (Couturier *et al.*, 1990) was subcloned as described previously (Revah *et al.*, 1991) into the pBluescript KS^+ vector to permit single-stranded DNA synthesis. Mutants were performed using an oligonucleotide-directed mutagenesis kit supplied by Amersham (Arlington Heights, IL).

Electrophysiological recordings. Perfusion solution was fed by gravity at a rate of ~6 ml/min. The oocytes were superfused continuously with OR2-Ba^{2+} (or OR2-Ca^{2+}), and solution exchange was controlled by computer-driven electromagnetic valves (Type III; General Valve, Fairfield, NJ). Electrophysiological recordings were made 2–4 days after the injection using a two-electrode voltage-clamp (GENECLAMP amplifier; Axon Instruments, Foster City, CA). Electrodes made from borosilicate glass were filled with a filtered solution of 3 M KCl. Unless specified, the holding potential was −100 mV. All experiments were performed at 18°.

Cell line, culture, and recordings. Human embryonic kidney cells (293 cells) transfected with a plasmid containing the human $\alpha7$ cDNA (K-28 cell line) were maintained in culture according to the method described previously (Gopalakrishnan *et al.*, 1995). Cells were plated onto 35-mm Petri dishes 2–5 days before recording. During electrophysiological experiments, cells were placed in a medium containing 120 mM NaCl, 5 mM KCl, 2 mM $MgCl_2$, 2 mM $CaCl_2$, and 10 mM HEPES, pH adjusted to 7.4 with NaOH. ACh-evoked currents were recorded using the whole-cell configuration of the patch-clamp technique. The intracellular solution contained 140 mM Cs-methanesulfonate, 5 mM NaCl, 2 mM $MgCl_2$, 10 mM BAPTA, and 10 mM HEPES, pH 7.4 adjusted with CsOH. In some experiments, 0.3 mM GTP (sodium salt) and 4 mM ATP (sodium salt) were added to the pipette medium as well as a regenerating system composed of 10 mM Na-phosphocreatine and 50 units/ml creatine phosphokinase. Pipettes were pulled from borosilicate glass and mounted on the head-stage of an AXOPATCH 200B amplifier (Axon Instruments). Drugs were applied using a liquid filament system based on a double barrel mounted on a piezoquartz actuator (Physics Instruments, Germany). In each side of the double barrel, a multitubing puffer (Bertrand *et al.*, 1997) was inserted to allow combined applications and fast drug exchange (within a few msec).

Data analysis and computation. Data were captured on-line by an analog-to-digital converter (AT-MIO16; National Instruments, Austin, TX) and stored on the hard disk of a personal computer for later analysis. Mathematical analysis and curve fitting were performed on a Macintosh using personal software based on a mathematical interpreter. Curve fitting was done using a least-squares minimization algorithm (SIMPLEX). Dose-response curves were adjusted using the empirical Hill equation:

$$y = \frac{1}{1 + \left(\frac{EC_{50}}{x}\right)^{n_H}} \quad (1)$$

where y is the fraction of activated current, EC_{50} is the concentration of half activation, n_H is the apparent cooperativity, and x is the agonist concentration.

Desensitization time constants were fitted with a single exponential and a constant in the form:

$$y = A_0 \cdot e^{-\left(\frac{t}{\tau}\right)} + B \quad (2)$$

where y is ACh-evoked current, A_0 is amplitude at time zero, t is time, τ is time constant, and B is plateau level.

Curve fitting with the two-state allosteric scheme was done using

the equation derived from the proposed Monod-Wyman-Changeux model (Monod *et al.*, 1965), written for the equilibrium conditions as:

$$B \xleftrightarrow{L} A$$

$$\bar{A} = \frac{1}{1 + L \cdot \left\{ \frac{1 + \frac{x}{K_B}}{1 + \frac{x}{K_A}} \right\}^n} \quad (3)$$

where A is a fraction of receptors in the active (open) state, x is agonist concentration, L is isomerization constant between B (basal) and A (active), K_A and K_B are intrinsic affinity constants, and n is the number of acetylcholine binding sites.

All values in the text are given as mean ± standard deviation.

Results

IVM potentiates the ACh-evoked response of the chick and human α7 nAChRs. The application of IVM alone evoked no detectable current in 176 oocytes expressing the chick α7 nAChR (currents <3 nA, Fig. 1A), even when concentrations as high as 300 μM were applied for >30 sec (data not shown). Similarly, no detectable modification of the ACh-evoked current was observed when 30 μM IVM was coapplied with ACh (Fig. 1A). In contrast, a clear increase in the ACh response was noticed after a 16-sec preapplication of IVM (30 μM, Fig. 1A). Recordings of responses to different ACh concentrations at control and after IVM preapplication (30 μM, 16 sec) revealed that this treatment caused a large increase in the subsequent ACh responses (Fig. 1B). Applications of a low ACh concentration (3 μM) evoked no detectable current in α7-expressing oocytes; however, when the same test pulse was applied subsequently to IVM, this low ACh concentration evoked a significant inward current. This result suggests that in addition to an increase in the current amplitude, IVM caused a shift toward a lower concentration of ACh dose-response curve.

To explore further the effects of IVM, ACh dose-response curves were established at control and after IVM preapplication. Normalized data obtained in seven cells over a broad

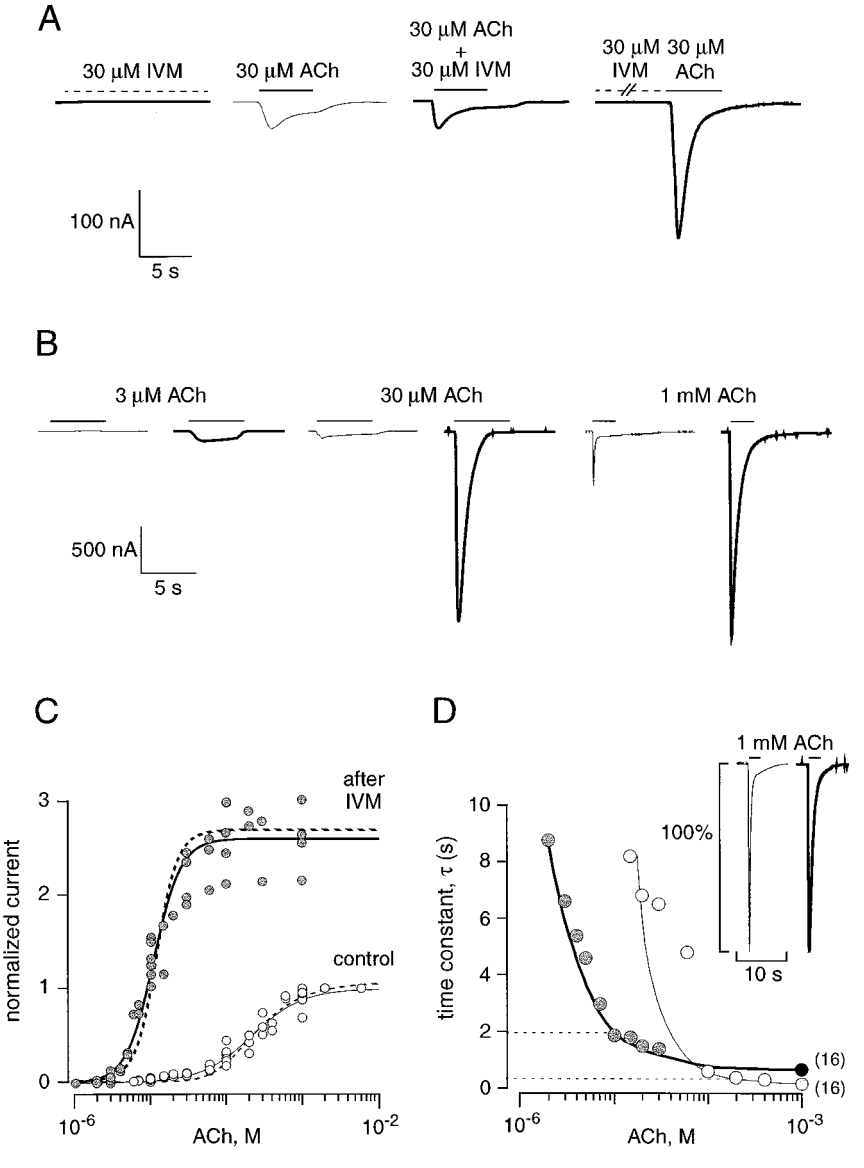

Fig. 1. IVM potentiates ACh-evoked current of the α7 nAChR. A (*Left to right*), IVM alone neither induces current nor affects the ACh-evoked current when coapplied with the agonist but strongly increases the subsequent ACh response if used as a preapplication (16 sec). *Dashed line*, IVM preapplications. B, Effects of IVM preapplication on currents evoked by different ACh concentrations. *Thin lines*, responses recorded in control conditions. *Thick lines*, responses obtained in the same cell after 16-sec IVM preapplication. C, Normalized dose-response curves recorded at control (○) and after IVM preapplication (●). Data obtained from seven cells were normalized to unity for the saturating values obtained in control conditions. *Lines through data points*, Hill equations (eq. 1) with respective values of EC_{50} = 216 μM, n_H = 1.3 (control) and EC_{50} = 11 μM and n_H = 2.5 (after IVM). *Dashed lines*, fits obtained with a two-state allosteric model (eq. 3) with respective coefficients of L = 10^6, K_A = 3.9 μM, and K_B = 56.8 μM (control) and L = 350, K_A = 3.9 μM, and K_B = 56.8 μM (after IVM) (five binding sites under each condition). D, Desensitization time constants obtained in a cell over the entire dose-response relationship are plotted as a function of the agonist concentration. Time constants were deduced by curve fitting using eq. 2. ○, Values obtained at control. ●, Time constant measured during IVM potentiation. (*Lines through data points* were drawn to aid the eye.) *Dashed lines*, time constant for the respective EC_{50} values. ●, Mean desensitization time constants measured at 1 mM ACh (n = 16). *Inset*, normalized currents evoked by 1 mM ACh in control (*thin line*) and after IVM (*thick line*) illustrating the difference in time constant. *Bars above current traces*, ACh application. Potentiation was obtained with preapplications of 30 μM IVM for 16 sec.

range of ACh concentrations are shown in Fig. 1C; this figure illustrates that IVM preapplication caused 1) an overall increase in ACh-evoked current amplitude [with a mean of 3 ± 1.31-fold at 1 mM ACh (n = 13)], 2) a shift toward a lower concentration of the half-maximal activation by ACh [from 176 ± 35 μM (n = 16) to 11 ± 3.4 μM (n = 11)], and 3) an increase in the apparent cooperativity, corresponding to an increase in the Hill coefficient [from 1.7 ± 0.2 (n = 16) to 3.1 ± 1.3 (n = 11)]. Dashed curves illustrate that IVM potentiation can be described on the basis of a two-state allosteric model (eq. 3) assuming that this compound acts as an allosteric effector that preferentially stabilizes the receptor in the active (A) state. Another important observation is that as shown in Fig. 1B, the desensitization time course of the ACh-evoked current was reduced by IVM preapplication. Further analysis was done to compare the time constants of desensitization at control and after IVM preapplication (Fig. 1D). Because of the left shift in the EC_{50} value and the overall increase in current amplitude, care must be taken when comparing the time constants; therefore, two critical points were used for the comparison: the time constants at the respective ACh EC_{50} values (*dashed lines*) and the values at saturation (1 mM). At the EC_{50} value (one cell), time constants of desensitization measured at control and after IVM preapplication were 0.38 and 1.9 sec, respectively. At 1 mM ACh, average time constants were 0.19 ± 0.098 (n = 16) and 0.65 ± 0.178 (n = 16) sec, respectively. These data illustrate that IVM exposure reduced the desensitization time course by ≥3-fold.

To assess the specificity of IVM potentiation, oocytes were injected with human α7 nAChR cDNA, and their properties were examined in experimental conditions identical to those described above. Performance of the experiments in sibling oocytes revealed that IVM was approximately equipotent on the chick or human α7 nAChR; namely, IVM preapplication resulted in a reduction in the ACh EC_{50} (Table 1). Concomitantly, and like for the chick α7 receptor, a significant reduction in desensitization time course was observed (Fig. 2A). The equipotency of IVM on human and chick receptors is illustrated clearly when comparing the current ratios measured before and after IVM preapplication at 30 μM ACh (Fig. 2B). These data indicate that IVM potentiation is not restricted to the chick α7 nAChR and that homologies between the avian and human receptors are sufficient to allow comparable potentiation.

IVM potentiation is independent of nonspecific Cl^- channel activation. It is well documented that α7 nAChR is highly permeable to Ca^{2+} (for a review, see Bertrand and Changeux, 1995) and that increase in the free Ca^{2+} concentration in the cytoplasm of the oocyte may trigger the activation of endogenous Cl^- currents that are sensitive to Ca^{2+} but much less to Ba^{2+}. Because IVM has been shown to activate Cl^--permeable channels (Schönrock and Bormann, 1993), we investigated whether the increase in ACh-evoked currents results from a direct action of IVM on the α7 nAChR or from a possible increase in the Cl^- contamination.

To examine the possible contribution of the endogenous Cl^- channels on the ACh-evoked currents, three approaches were used: 1) determination of IVM potentiation in an external solution containing Ba^{2+} instead of Ca^{2+}, 2) measurements of the reversal potential of the ACh-evoked current at control and after IVM preapplication, and 3) investigation of the potentiation of the Ca^{2+}-impermeant mutant α7-E237A (Bertrand *et al.*, 1993).

Because Ca^{2+}-activated Cl^- channels are ~50 times less sensitive to Ba^{2+} than to Ca^{2+}, exchange of these two divalent cations in the extracellular medium is a standard maneuver to minimize the possible contribution of Cl^- currents. Determination of the ACh dose-response relationships in Ba^{2+}-containing medium showed that IVM was as effective as in the presence of extracellular Ca^{2+} ; therefore, most experiments were performed with Ba^{2+}-containing medium.

To determine the influence of IVM on the reversal potentials, I-V curves were measured at control and after IVM preapplication. However, to enhance the differences between the reversal potentials for cations (α7 ACh-evoked current) and Cl^-, responses were recorded in a medium in which Cl^- ions were substituted by the impermeant anion gluconate (Galzi *et al.*, 1992). Reversal potentials of the cationic and Cl^- channels estimated under these conditions would be −10 and +40 mV, respectively. I-V curves were measured by plotting the peak of the responses evoked by short applications of ACh near the EC_{50} value (100 μM, 2 sec) as a function of the holding potential between −50 and +10 mV. Results shown in Fig. 3A illustrate that IVM caused no detectable changes in the ACh-evoked current reversal potential. The mean reversal potential measured in control was −14.8 ± 0.4 mV (n = 4), whereas a value of −14 ± 0.4 mV was determined in the same cells after IVM application (30 μM, 16 sec).

Mutation of a single amino acid at the inner mouth of the α7 channel was found to be sufficient to reduce its Ca^{2+} permeability to an undetectable level (Bertrand *et al.*, 1993). Consequently, ACh-evoked currents recorded in this mutant display no contamination by Cl^- channels. This was illustrated by the shift of the I-V curve toward the potassium equilibrium observed on substitution of the extracellular sodium with an equimolar concentration of Ca^{2+} (Bertrand *et al.*, 1993). Data presented in Fig. 3B illustrate that mutant α7-E237A is strongly potentiated by IVM. The apparent EC_{50} value was shifted ~10-fold (Table 1; data were measured for

TABLE 1

Apparent ACh sensitivities of the α7 nAChRs and mutants before and after ivermectin treatment

Values in parenthesis correspond to the number of cells tested in each condition. All measurements were performed at −100 mV.

cDNA type	Control		After IVM		EC_{50} (control)
	EC_{50}	n_H	EC_{50}	n_H	EC_{50} (after IVM)
	μM		μM		
Human α7 WT	180 (2)	1.2 (2)	9 (2)	3.0 (2)	20
Chick α7 WT	176 ± 35 (16)	1.7 ± 0.2 (16)	11 ± 3.4 (11)	3.1 ± 1.3 (11)	16
Chick α7 E237A	180 (2)	1.6 (2)	21 (2)	2.0 (2)	8.6
Chick α7 L247T	1.64 ± 0.84 (6)	1.6 ± 0.8 (6)	1.45 ± 0.71 (6)	2.0 ± 0.4 (6)	1.1
Chick α7 V251T	0.84 ± 0.56 (6)	2.4 ± 0.3 (6)	0.21 ± 0.15 (6)	1.9 ± 0.5 (6)	4.0

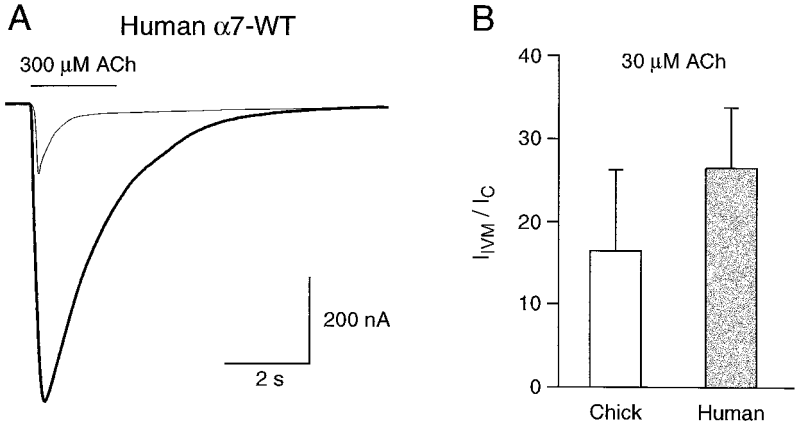

Fig. 2. Potentiation of the human α7 nAChR. A, Currents evoked by an ACh concentration, near the EC_{50}, showing a strong increase after IVM preapplication. *Thin line*, control. *Thick line*, obtained in the same cell after IVM preapplication (30 μM, 16 sec). B, Comparison of the potentiation of the ACh-evoked current (at 30 μM ACh) of the chick and human α7 nAChR. Ratios were computed as I_{IVM}/I_C, with I_{IVM} and I_C corresponding to the current values (in nA) recorded after IVM or at control, respectively. Mean ratios were 16.5 ± 9.5 (n = 24) for chick α7 and 26.5 ± 7.2 (n = 4) for human α7.

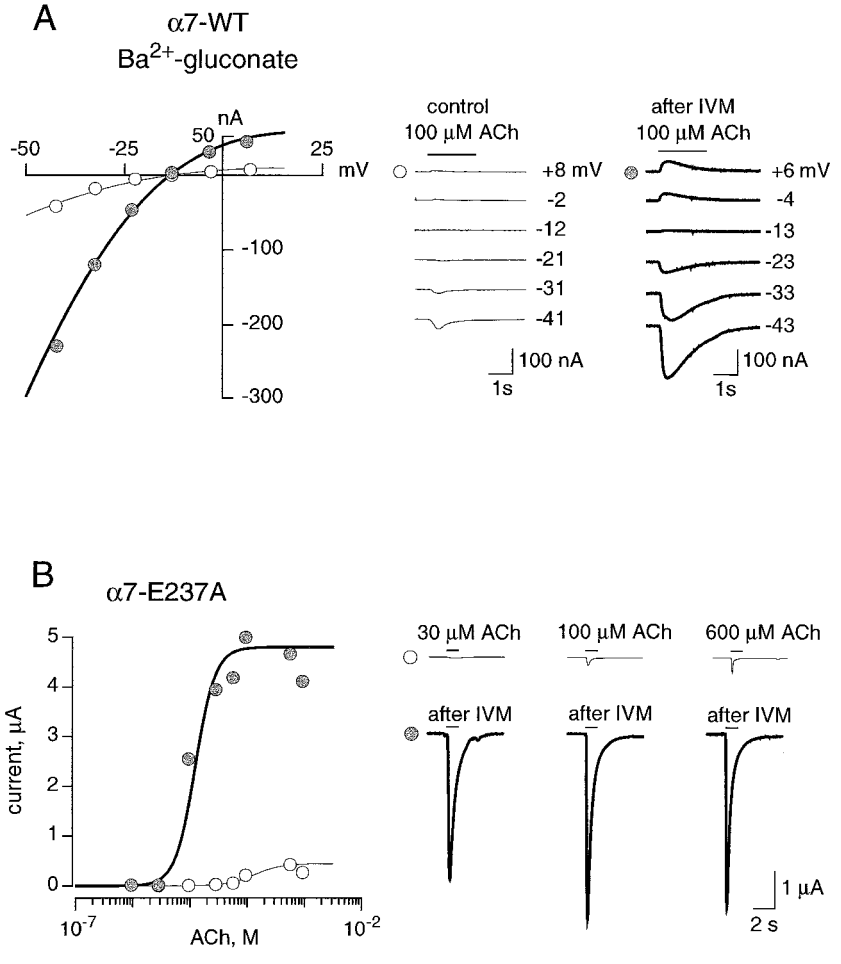

Fig. 3. IVM potentiation is independent of Cl^- channels. A, I-V relationships were determined by measuring the ACh-evoked current (100 μM, 2 sec) at different holding potentials. *Right*, time courses of the currents. To enhance the difference between the ACh-evoked current reversal potentials and Cl^- equilibrium, Cl^- was partially substituted by gluconate. B, The α7 mutant E237A is strongly potentiated by IVM. *Left*, ACh dose-response relationship measured before and after IVM preapplication (same protocol as in Fig. 1C). Right, corresponding currents. ○, Control. ●, Currents recorded after IVM preapplication (1 μM, 16 sec).

16-sec preapplication of 1 μM IVM) with a 10-fold increase in the saturation response. The effects always were accompanied by a reduction in desensitization. Taken together, these data clearly illustrate that IVM potentiation still is observed after removal of Cl^- contamination and is in agreement with a direct action of IVM on the α7 receptor.

Kinetics of IVM action. Preliminary experiments revealed that short exposure to IVM produces little or no potentiation of the subsequent ACh-evoked currents. To examine in more detail the relationship between the duration of IVM preapplication and the subsequent current potentiation, a fixed concentration of both IVM (30 μM) and ACh (60 μM) was used, and the duration of the IVM prepulse was increased gradually from 1 to 128 sec. After each test, cells were superfused with control solution until recovery of their initial response. Fig. 4A illustrates the results obtained with three cells. These data show that potentiation follows a sigmoidal relationship and becomes significant only for preapplications of >4 sec. Maximal potentiation corresponded to ~14-fold of the initial response (at 60 μM ACh) and was reached within 2 min. However, due to technical reasons, a 16-sec IVM preapplication usually was used. This caused an average 4.1 ± 1.47-fold potentiation (at 60 μM ACh, n = 10) of the initial ACh-evoked current. At higher IVM concentra-

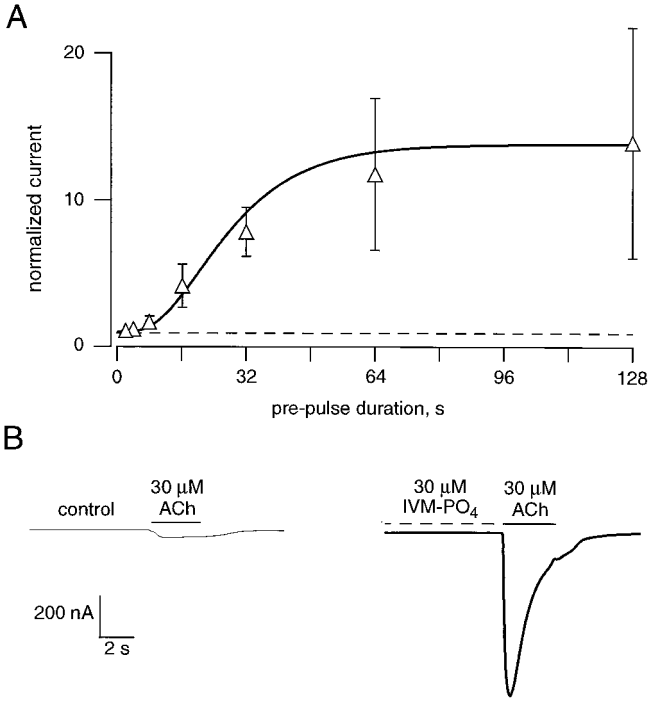

Fig. 4. IVM mode of action. A, Potentiation by IVM is time dependent. Peak currents evoked by a fixed ACh pulse (60 μM, 2 sec) are plotted as a function of the duration of IVM (30 μM) preapplication. Values are mean ± standard deviation from three cells. (*Sigmoidal line through data points* was added to support the eye.) B, Water-soluble form of IVM phosphate potentiates the ACh-evoked currents. *Traces* correspond to currents evoked at control (*thin line*) and after a 6-sec pulse of IVM-PO_4 (*thick line*). *Bars*, ACh application.

tions, effects could last as long as 20 min. For lower IVM concentrations, recovery of the response amplitude and time course was observed within a shorter time (data not shown).

IVM effects are not mediated by the membrane. Because of the lipophyllic character of IVM, it was suggested that this compound partitions in the lipid bilayer (Campbell, 1989) and, as a consequence, modifies the receptor environment. To test this possibility, we examined the effects of the water-soluble IVM-PO_4 on ACh-evoked currents. As shown in Fig. 4B, a 6-sec prepulse of IVM-PO_4 potentiates ACh-evoked currents. A reduction in desensitization comparable to that caused by IVM also was observed. Moreover, when an equivalent concentration and application time of IVM-PO_4 and IVM were used on the same cell, the water-soluble form caused a more important potentiation than the lipophyllic compound. These results are consistent with a direct action of this compound as an allosteric effector of the α7 nAChRs.

Effects of IVM on the response of α7 nAChR to a partial agonist. To evaluate further the possibility that IVM acts as an allosteric effector of the α7 neuronal nAChRs [e.g., by stabilizing its active (open) conformation], the effect of IVM on the dose-response curve of a partial agonist was investigated. We selected DMPP, which behaves as a partial agonist of the chick α7 nAChR, evoking ~1–10th of the maximal response to ACh (average of 13.2% in four cells) (Bertrand *et al.*, 1992; Peng *et al.*, 1994). Fig. 5A illustrates that after IVM preapplication, DMPP becomes almost a full agonist. The ratio of DMPP to ACh-evoked current of 65 ± 6.7% was measured in five cells. In agreement with the observations presented here, both ACh and DMPP responses showed a significantly slower time course after IVM exposure. The apparent affinity increased on average by only 1.7-fold (from 14.2 to 8.5 μM, $n = 4$) for DMPP (instead of 16-fold, as determined for ACh; Table 1) after preapplication of IVM. Similar potentiation of partial agonists by allosteric effectors has been reported extensively in the past with allosteric enzymes (Monod *et al.*, 1965) and discussed in the framework of nAChR mutants (Galzi *et al.*, 1996).

Effects of a competitive inhibitor on IVM potentiation. MLA is a high affinity blocking agent of the homomeric α7 nAChR that displays an IC_{50} value for this compound in the picomolar range (Palma *et al.*, 1996). Compelling evidence indicates that MLA competes with ACh and inhibits the response by stabilizing the receptor in a closed state (Wonnacott *et al.*, 1993; Bertrand *et al.*, 1997). To determine whether MLA interacts with IVM, potentiation experiments were conducted before, during, and after MLA blockade. Typical results obtained with the Ca^{2+}-impermeant mutant E237A receptor are presented in Fig. 5B. These data illustrate that incubation in presence of a MLA concentration sufficiently high to suppress the ACh-evoked current also abolishes IVM potentiation (*middle trace*). Full recovery of both the ACh-evoked current and IVM potentiation were obtained readily after a 19-min wash (Fig. 5B, *right traces*). Similar data have been obtained with the wild-type receptor (data not shown).

Mutations in the channel domain alter IVM potentiation. The putative allosteric effects of IVM also were examined on chick α7 receptors mutated at two distinct locations (V251T and L247T) in the second transmembrane segment, TM2. As shown previously, these mutations produce pleiotropic effects on the receptor properties with an increase in apparent affinity, a loss of desensitization, and alteration of agonist-versus-antagonist profile (Revah *et al.*, 1991; Devillers-Thiéry *et al.*, 1992; Bertrand and Changeux, 1995). Furthermore, it was shown recently that in the L247T mutant, a fraction of the nAChR is spontaneously open (Bertrand *et al.*, 1997). As illustrated in Fig. 6, IVM affected the two mutants expressed in *X. laevis* oocytes in a strikingly different manner. Preapplication of IVM on oocytes expressing the V251T mutant provoked a small (6.4 ± 2%, $n = 7$) but consistent increase in the leakage current in the absence of agonist. It is important to note that in every cell tested, this increased leak current is suppressed readily by the application of MLA (data not shown). In addition, however, a small but consistent reduction in the maximal ACh-evoked current was observed after IVM preapplication. Determination of the ACh dose-response relationship, over a broad range of agonist concentration, of this mutant before and after IVM exposure revealed a significant increase in the apparent affinity of ~5-fold (Fig. 6A, *left*, and Table 1). No significant modification of the time course of the ACh-evoked current was noticed after IVM exposure (Fig. 6A, *right*). As in the case of the wild-type receptor (Fig. 1C), dose-response curves can be fitted with the two-state allosteric model (eq. 3). A multiplying factor that was inferior to unity was, however, introduced to describe the smaller amplitude of responses recorded after IVM exposure. In contrast, when the experiments were repeated in oocytes expressing the L247T mutant, a different pattern was observed (Fig. 6B). First, IVM strongly reduced the amplitude of the ACh-evoked current at every concentration tested; second, the apparent affinity for ACh remained unchanged

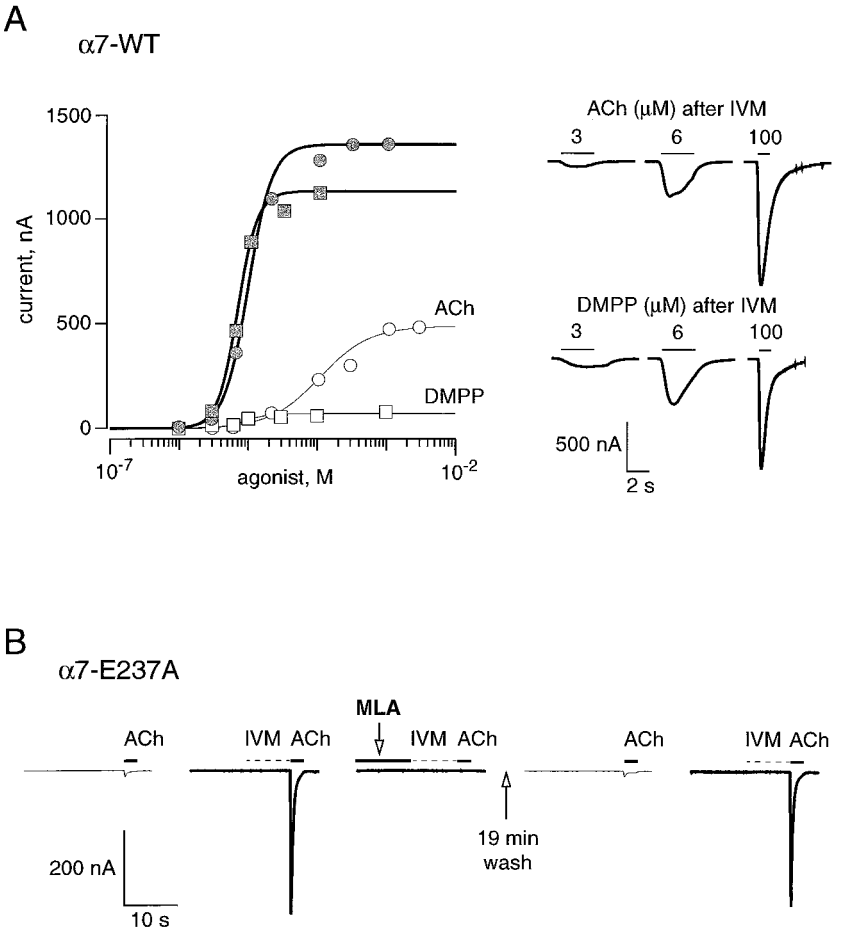

Fig. 5. Pharmacological properties of the IVM-potentiated responses. A, IVM changes the pharmacological profile of DMPP. The chick α7 partial agonist DMPP efficiency is strongly increased after IVM (30 μM, 16 sec) preapplication, as shown from both the dose-response relationship (*left*) and individual currents (*right*). Dose responses were measured and plotted as for Fig. 1C. ○, □, Control. ●, ■, Obtained after IVM preapplications. *Lines through data*, correspond to the empirical Hill equations with respective EC_{50} values and Hill coefficients of 110 μM and n_H = 1.2 (ACh control), 10 μM and n_H = 2.5 (ACh after IVM), 9 μM and n_H = 2.7 (DMPP control), and 7 μM and n_H = 3 (DMPP after IVM). B, Blockade of the α7-E237A receptor by the competitive inhibitor MLA. ACh-evoked currents (ACh = 60 μM) recorded in a medium containing 2.5 mM Ca^{2+} before and after IVM preapplication (30 μM, 8 sec) were recorded first at control and after a 10-sec exposure to 10 μM MLA (*thick line*). This MLA exposure is sufficient to fully inhibit ACh-evoked currents under both conditions. Parallel recovery of the responses and their potentiation always was observed. The cell was held at −100 mV throughout the experiment.

(Fig. 6B, *left*, and Table 1). Also, IVM exposure did not significantly increased the leak current. Furthermore, as in the case of the V251T, no modification of the response time course was detected for the L247T mutant (Fig. 6B, *right*).

IVM potentiates responses of the human α7 nAChR expressed in human embryonic kidney 293 cells. To further evaluate the time course of IVM action and rule out effects specific to the oocyte system, we examined the effects of IVM on K-28 cells expressing the human α7 nAChR (Gopalakrishnan *et al.*, 1995). The application of IVM alone induced no detectable current in every cell tested (n = 15). Traces presented in Fig. 7 illustrate that preapplication of 25 μM IVM elicited a significant increase in the current evoked by low ACh concentration (30 μM). Although a clear potentiation already was observed after a 1-sec exposure, the maximal effect was obtained with 5–10-sec preapplications. Complete recovery of both amplitude and time course of the ACh-evoked currents was observed within 2–5 min, depending on the duration of the IVM prepulse. Moreover, data presented in Fig. 7 show that potentiation and recovery can be repeated several times in a same cell.

To compare further the results from cell line with those obtained from *X. laevis* oocytes, we determined the effects of IVM on the ACh dose-response curve. The plots of the peak ACh-evoked currents measured in one cell before and after IVM preapplication yielded data presented in Fig. 8A. In agreement with data obtained from *X. laevis* oocytes, IVM causes an increase in the apparent affinity to ACh (from 120 to 30 μM) that is accompanied by an increase in the apparent cooperativity evaluated with the Hill coefficient (from 1.6 to 1.8). Examination of the time course of the ACh-evoked currents (Fig. 8B) reveals that concomitant to potentiation, a marked decrease of receptor desensitization time course is observed. Both of these effects were fully reversible within a couple of minutes. Partial ACh dose-response curves presenting similar potentiation were obtained in several cells (n = 7, data not shown). Unlike the data obtained on oocytes, IVM preapplication produces little modification of the maximal ACh-evoked current; however, further work is needed to confirm the possible significance of such difference.

The water-soluble form of IVM (IVM-PO_4) was found to potentiate responses in *X. laevis* oocytes. Similarly, IVM-PO_4 was found to be more potent on K-28 cells, as illustrated by data presented in Fig. 8, C and D. The mean potentiations at 30 μM ACh were 3.46 ± 0.53 (n = 6) and 4.75 ± 1.07 (n = 4) for 25 μM IVM and 10 μM IVM-PO_4, respectively. The time course of IVM-PO_4 potentiation as well as its recovery were comparable to those observed for IVM.

Discussion

The data presented in this work demonstrate that the anthelmintic drug IVM strongly potentiates the ACh-evoked current of the α7 homomeric neuronal nAChRs from both chick and human.

IVM is a semisynthetic analog of the natural compound avermectin that contains ≥80% 22,23-dihydroavermectin B1a and ≤20% of the B1b homologue (Campbell, 1989). Aver-

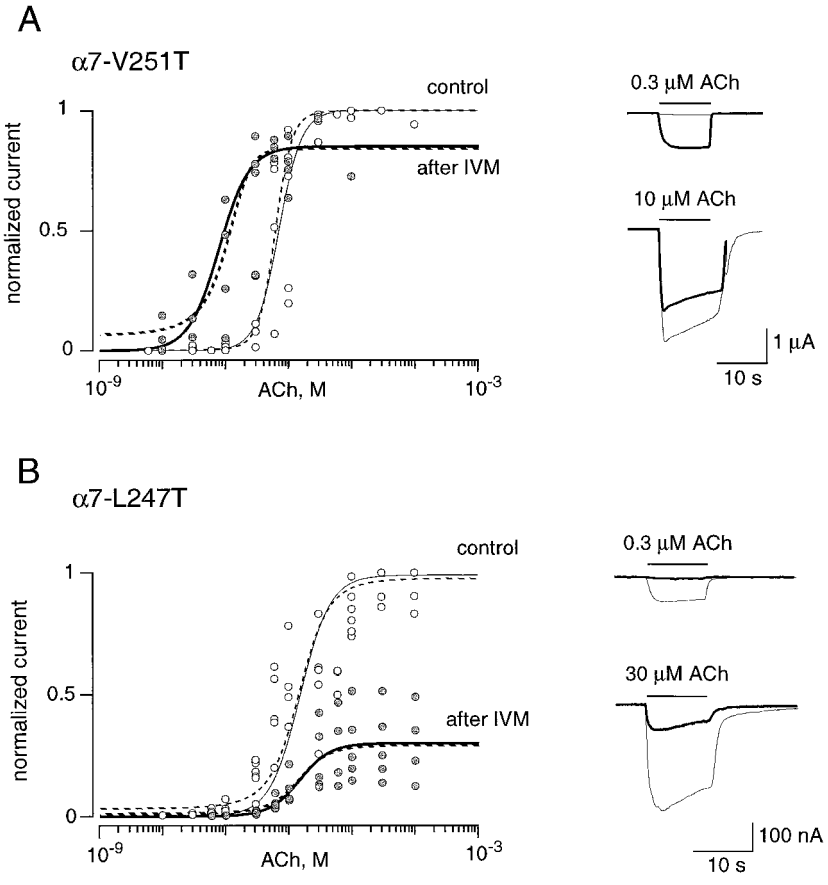

Fig. 6. IVM potentiation distinguishes TM2 mutants. Effects of IVM preapplication on oocytes expressing the α7-V251T (A) and α7-L247T (B) mutants. Dose-response curves were obtained using the same protocol presented in Fig. 1C. *Lines through data points*, correspond to the Hill equations with respective EC_{50} values and Hill coefficients of 0.7 μM and n_H = 2.4 (α7-V251T control, n = 6) 0.08 μM and n_H = 1.8 (α7-V251T same cells, after IVM) 1.55 μM and n_H = 1.8 (α7-L247T control, n = 6) 1.55 μM and n_H = 1.8 (α7-L247T same cells, after IVM). *Dashed lines*, fits obtained with a two-state allosteric model (eq. 3) with respective coefficients L = 1800, K_A = 0.14 μM, and K_B = 3.1 μM (control) (five binding sites), whereas L = 12 (after IVM) for the V251T. Values of L = 30, K_A = 0.8 μM, and K_B = 3.3 μM (five binding sites) were used for the L247T both at control and after IVM. A scaling factor of 0.3 was added to take into account the lower current amplitude of L247T mutant after IVM. Right, individual currents recorded before and after IVM. *Thin lines*, control. *Thick lines*, recordings obtained after IVM preapplication (30 μM, 15 sec for α7-V251T; 10 sec for α7-L247T).

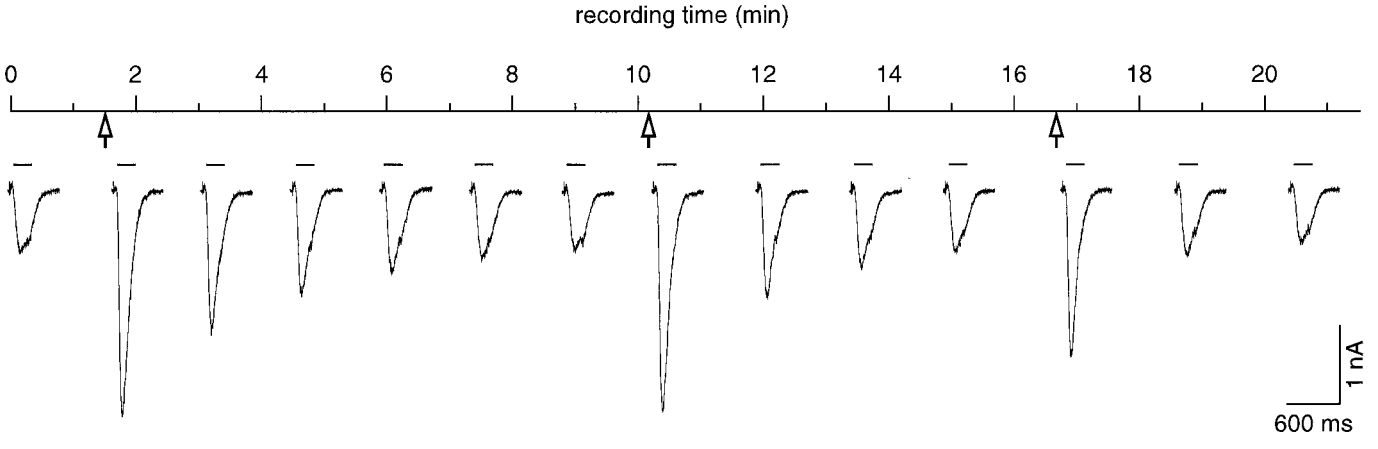

Fig. 7. Time course of IVM potentiation and recovery in K-28 Cells. ACh-evoked currents measured in whole-cell configuration were recorded at regular intervals. The cell was maintained in voltage clamp at −100 mV and challenged with 200-msec pulses of 30 μM ACh (*small horizontal bars*). The application of a short IVM pulse (25 μM, *arrows*) induced no current deflection (not shown) but provoked a strong potentiation of the ACh-evoked currents. Complete and readily reversible, potentiation could be induced by successive IVM prepulses. *Left to right* (*arrows*), IVM pulse durations of 30-, 20-, and 5-sec, respectively.

mectin was isolated ~20 years ago from the soil bacterium *Streptomyces avermitilis* in a large scanning of natural substances with anthelmintic activity (Burg *et al.*, 1979). In humans, IVM has been considered the drug of choice for the treatment of river blindness (for a review, see Ottesen and Campbell, 1994). River blindness (Onchocerciasis), which affects ~21 millions persons in the world, is caused by infection with the filarial nematode *Onchocerca volvulus* (Mahmoud, 1995). A single oral administration of IVM in a standard dose of 150 μg/kg of body weight has been shown to rapidly eliminate microfilariae (Pacqué *et al.*, 1991) with a very low rate of adverse reactions. The mechanism of action of IVM remains to be elucidated.

Recently, an avermectin-sensitive glutamate-gated Cl^- channel displaying an important structural homology with the nAChR subunits was identified and cloned from *Caenorhabditis elegans* (Cully *et al.*, 1994). In addition, IVM has been reported to potentiate, in an allosteric manner, ligand-gated channels activated by GABA (Sigel and Baur, 1987; Krusek and Zemková, 1994). These observations prompted

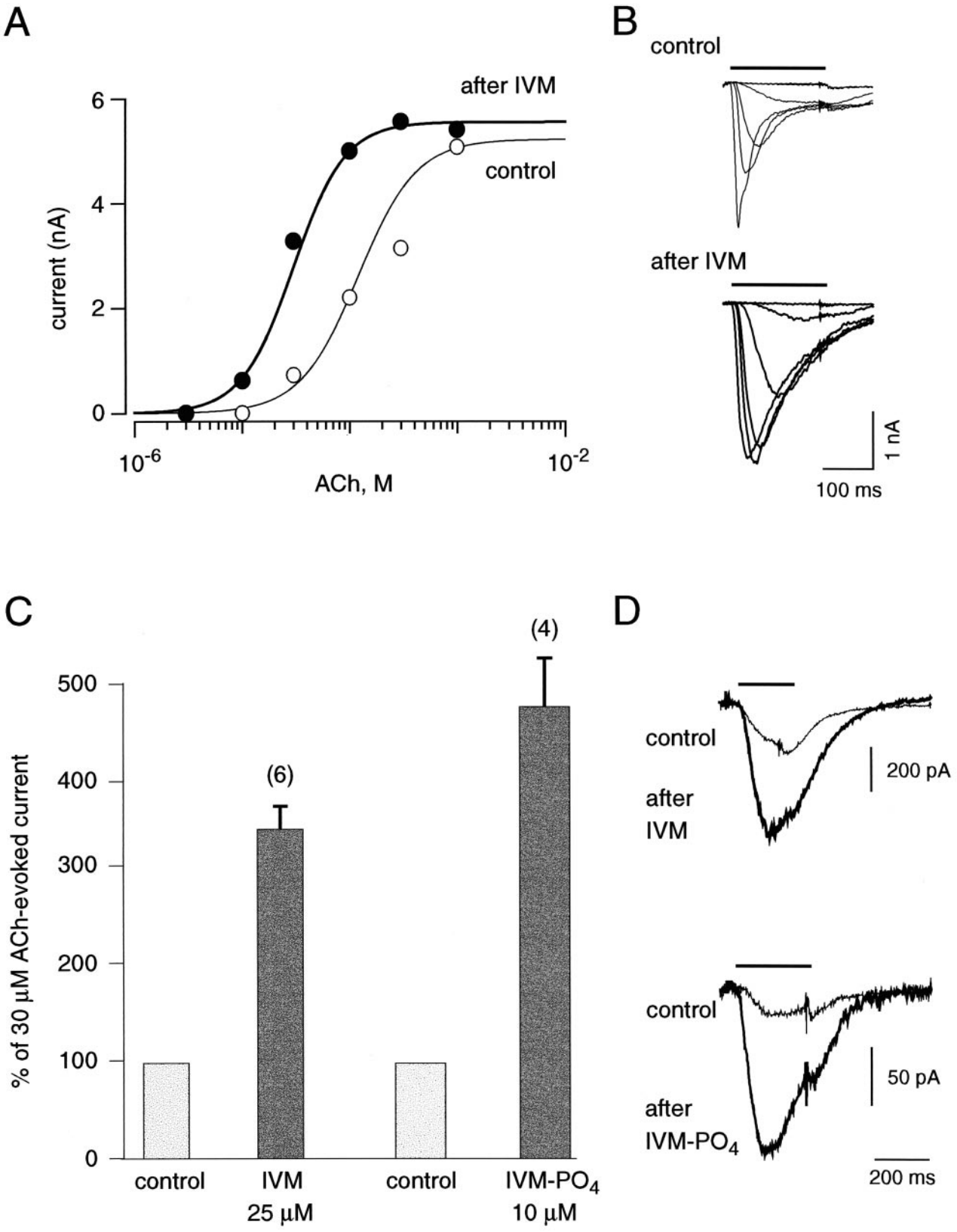

Fig. 8. IVM and IVM-PO_4 potentiate the human α7 nAChR in K-28 cells. A, Apparent agonist affinity of a single cell was determined using 200-msec pulses of ACh concentrations applied in a growing order first in control solution and then in the presence of 25 μM IVM prepulse. Fit of the data with the empirical Hill equation yielded an apparent affinity of 120 μM and Hill coefficient of 1.6. In the presence of IVM prepulses, these values shift to 30 μM and 1.8, respectively. B, Currents evoked by increasing ACh concentrations (3, 10, 30, 100, 300, and 1000 μM; *horizontal bars*) under control conditions and after IVM prepulses (same as in A) are superimposed. C, Mean potentiations induced by IVM and IVM-PO_4 were 3.46 ± 0.53 and 4.75 ± 1.07, respectively. IVM prepulse was ~10 sec. D, Currents evoked by a 30 μM ACh concentration (*horizontal bar*) at control and after a 10-sec prepulse of IVM (or IVM-PO_4).

us to investigate the effects of IVM on neuronal nAChRs using the functional α7 neuronal nAChR.

We found that a preapplication of micromolar concentrations of IVM markedly increased the current evoked by a subsequent application of ACh, thereby causing a 20-fold shift of the apparent affinity of ACh. Concomitantly, in every cell tested, the Hill coefficient of the dose-response curve increased. Similar IVM sensitivity and potentiation of the ACh-evoked current were observed in receptors reconstituted with either the human or chick α7 nAChR subunits.

None of the IVM effects can be accounted for by an indirect activation of Ca^{2+}-activated Cl^- currents. Furthermore, given the important potentiation of the water-soluble form of IVM (IVM-PO_4), it is unlikely that IVM effects result from perturbation of the lipid bilayer organization of the membrane.

Based on the repeatability of the IVM potentiation observed on the α7 ACh-evoked currents both in *X. laevis* oocytes and in K-28 cells, it seems unlikely that IVM potentiation can be explained by the incorporation in the plasma membrane of new nAChR proteins from an internal store. As a correlate, this hypothesis would include the assumption that such a freshly expressed pool must be withdrawn from the plasma membrane every time IVM is removed. Finally, this hypothesis could not explain either the modification of the kinetics of the ACh-evoked responses or changes in the pharmacological profile.

The most likely interpretation of the presented results is that IVM acts on the α7 nAChR as a positive allosteric effector of the neuronal nAChR. This interpretation is reinforced by the observation that a modification of the pharmacological profile accompanies IVM potentiation. For example, DMPP, which behaves as a partial agonist of the chick α7 nAChR (Bertrand *et al.*, 1992; Peng *et al.*, 1994), becomes almost a full agonist after IVM preapplication, as anticipated for a positive allosteric effector that would stabilize the active open state. A similar conclusion was reached in previous attempts to model the kinetic properties of the α7 nAChR mutants on the basis of allosteric mechanisms (Galzi *et al.*, 1996b).

Moreover, site-directed mutagenesis experiments carried out within the TM2 channel domain previously revealed that substitutions of Leu247 or Val251 by a threonine profoundly modify α7 nAChR properties (Revah *et al.*, 1991; Devillers-Thiéry *et al.*, 1992). Both mutations cause an increase in the apparent affinity to ACh and a loss of desensitization. They have been interpreted in terms of differential alteration of the states and conformational equilibria of the nAChR: a selective permeabilization of the desensitized state for L247T and a modification of the equilibrium constant L between basal and active states for V251T (Galzi *et al.*, 1996b). The positions of these two mutations within the channel domain are shown in Fig. 9A.

Consistent with the notion that IVM potentiates nicotinic receptor responses by shifting the conformational equilibrium in favor of the active state, it still potentiates the V251T mutant but no longer affects the L247T mutant (Fig. 9B). Furthermore, in oocytes expressing the V251T mutant, the current leakage is increased by IVM, and this current can be blocked by MLA. This indicates that on the V251T mutant, IVM behaves as a positive allosteric effector.

These experimental data can be interpreted in terms of a

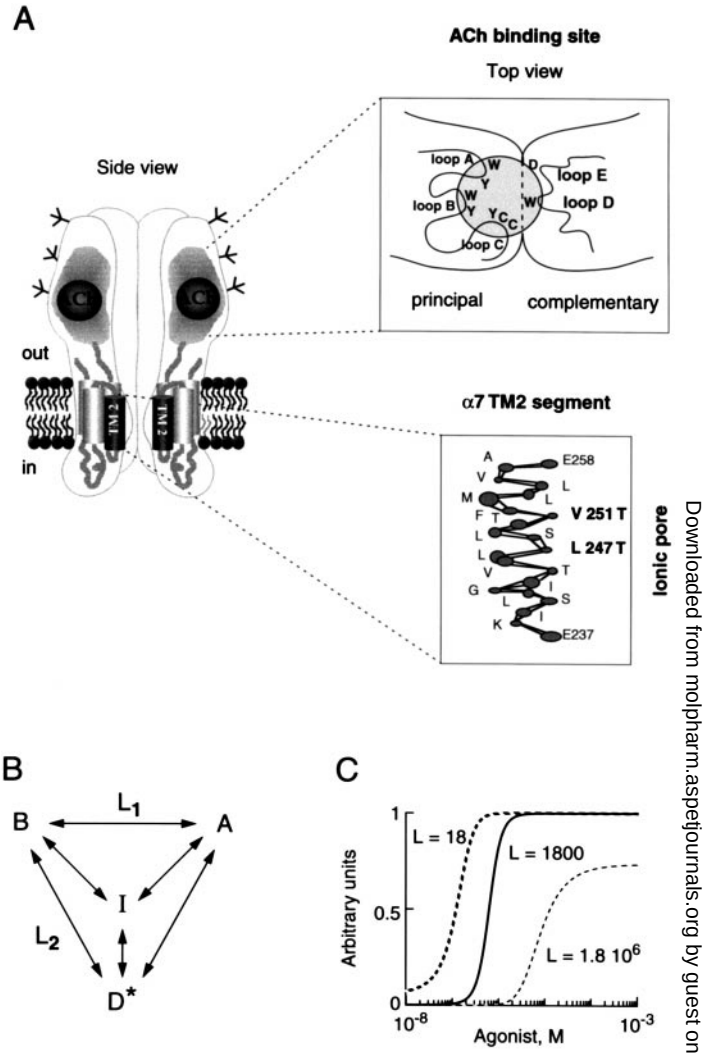

Fig. 9. Schematic of the nAChR and allosteric reactions. A, Side view of a schematic representation of the nAChR inserted in the membrane. *Right*, putative protein arrangement of one of the ACh binding site and the channel pore. Main and complementary loops participating in the formation of the ACh binding site are illustrated. *Channel inset*, point mutations (V251T and L247T). B, Allosteric reaction scheme including four states is shown where *B* is basal (closed) state, *A* is active (open) state, *I* is intermediate (closed) state, and *D* is desensitized closed state. L_1 and L_2 are the respective isomerization constants for the transitions from the B-A and/or B-D states. C, Dose-response curves computed from a two-state allosteric model (eq. 3) corresponding to the activation from *B* to *A* with different L values comparable to those predicted for (*right* to *left*) the wild-type and V251T and V251T after IVM preapplication. K_A = 0.14 μM, K_B = 3.1 μM, and five binding sites.

minimal two-state allosteric model (Monod *et al.*, 1965). The equilibrium constant (L value) describing the equilibrium between the basal (B) and active (A) states can be set to 12 (for the V251T, see Fig. 6) in the presence of IVM to account for ~8% of the maximal ACh-evoked current. Fig. 9C shows that changing only the L value may result in a slight agonistic effect of IVM on the V251T. Indeed, a high value of L, as may be the case for the wild-type receptor, would lead to a low apparent affinity receptor with no spontaneous or IVM-evoked, channel opening. The V251T mutation then would lead to a significant reduction in L (~1000), thus leading to an increased apparent affinity for agonist together with higher cooperativity and higher response amplitude (Galzi *et*

al., 1996b). The action of a positive allosteric effector such as IVM, according to Rubin and Changeux (1966), would correspond to a reduction in the L value and lead to detectable leak currents in the absence of acetylcholine and higher apparent affinity and response cooperativity in the presence of acetylcholine.

Such an interpretation also is in agreement with the data obtained on the L247T mutant receptor. Indeed, according to the interpretation proposed previously (Revah *et al.*, 1991; Galzi *et al.*, 1996b), the channel of the L247T mutant would become open in the desensitized conformation, and the equilibrium constants between the conformational states would not be altered. Thus, if IVM reduces the equilibrium constant between the basal (B) and active (A) states, its effect would become detectable only at the high agonist concentrations required to stabilize the active state and should not be observed at the concentrations that stabilize the desensitized but conducting state.

These data therefore document and demonstrate further that the V251T and L247T mutations differentially alter the properties of the allosteric states and conformational equilibria of the α7 nAChR, and, as a consequence, their responsiveness to IVM potentiation.

The high affinity displayed by the α7 nAChR for IVM and its water-soluble form IVM-PO_4 supports the view that this receptor carries a specific site that recognizes this type of pharmacological ligand. Experiments performed in a normal versus a low Ca^{2+} concentration showed that IVM causes a similar increase in apparent affinity under the two conditions (data not shown). Therefore, it seems unlikely that IVM enhances nAChR responses through the Ca^{2+} binding sites. Alternatively, IVM and steroids might modulate receptor activity through the same or overlapping sites. However, steroids have been shown to inhibit rather than to activate the α7 nAChR (Buisson and Bertrand, 1998), leaving the possibility that these two sites are distinct.

The slow time course observed for both the onset and recovery of IVM effects on *X. laevis* oocytes can reflect either a slow kinetic of action or a restriction of diffusion of this compound across the vitelline membrane. The time course of potentiation and recovery observed in K-28 cells suggests that IVM diffusion might be a limiting factor in the oocyte system.

The existence of a specific site allowing the binding of an allosteric effector does not necessarily imply the existence of an endogenous natural ligand, as shown for the bezafibrate site on hemoglobin (Perutz *et al.*, 1986). Thus, although IVM may interact with a specific domain of the protein, this drug may cause an allosteric potentiation comparable to that produced by a physiological but yet unknown compound that binds to another site.

At this stage, the possibility that IVM indirectly potentiates nAChRs through the activation of a second messenger system cannot be excluded totally. Experiments with K-28 cells expressing the human α7 nAChR (Gopalakrishnan *et al.*, 1995) revealed that IVM potentiation is not restricted to *X. laevis* oocyte but can be observed equally in another preparation. Thus, if IVM is acting through a specific receptor in the cell membrane, such a receptor should be expressed by cells as different as the oocyte and human embryonic kidney cells. Moreover, the effect of IVM on the human α7 nAChR expressed in K-28 cells was not modified by the addition of GTP plus an ATP-regenerating system into the pipette solution (see Materials and Methods). Potentiation also was independent of the addition of the chelating agent BAPTA in the intracellular medium. Thus, it is very unlikely that IVM effects are mediated by a second messenger system such as intracellular Ca^{2+} signaling, G protein pathway, or a kinase/phosphatase pathway.

Given the slow time course of agonist application in the oocytes and the fast desensitization of the α7 nAChR, it can be argued that partial masking of the ACh-evoked response occurs in this system. However, this interpretation does not apply for experiments with the K-28 cells, in which agonist application is performed within milliseconds. Furthermore, although this hypothesis could have taken into account the current increase observed at a high ACh concentration, it does not explain adequately the important shift in apparent ACh affinity observed for low nondesensitizing agonist concentrations. Finally, a strong argument in favor of the allosteric modulation is the modification of the pharmacological profile observed for the partial agonist DMPP, which cannot be explained on the basis of desensitization.

The strong potentiation caused by IVM on α7 nAChR seems to be reminiscent of the allosteric modulation of $GABA_AR$ by benzodiazepines or barbiturates (for a review, see Rabow *et al.*, 1995). Benzodiazepines were shown to modify the probability of channel opening, whereas barbiturates increased the mean open time (Puia *et al.*, 1990). From these observations, it was concluded that benzodiazepines act by modifying the allosteric isomerization coefficient L, whereas barbiturates are thought to alter the transition from liganded closed state to the open state (Rabow *et al.*, 1995). In this context, the effects caused by IVM resemble those of benzodiazepines on the $GABA_AR$ and are consistent with a reduction in the L coefficient.

In conclusion, we propose that IVM behaves as an allosteric effector that binds to a specific site on the α7 nAChR that is distinct from either the Ca^{2+} (or steroid) regulatory sites. Studies of pharmacological agents that act as allosteric modulators of the nAChRs may lead to the design of new types of compounds that could compensate the deleterious effects of neurodegenerative disorders such as Alzheimer's or Parkinson's diseases.

Acknowledgments

We thank Drs. S. P. Arneric, J. P. Sullivan, and M. Gopalakrishnan (Abbott Labs, Abbott Park, IL) for kindly providing the K-28 cells. Human α7 cDNA was kindly provided by Prof. J. Lindstrom.

References

Bertrand D, Bertrand S, and Ballivet M (1992) Pharmacological properties of the homomeric *alpha* 7 receptor. *Neurosci Lett* **146:**87–90.

Bertrand D, Buisson B, Krause RM, Hu H-Y, and Bertrand S (1997) Electrophysiology: a method to investigate the functional properties of ligand-gated channels. *J Recept Signal Transd Res* **17:**227–242.

Bertrand D and Changeux JP (1995) Nicotinic receptor: an allosteric protein specialized for intercellular communication. *Semin Neurosci* **7:**75–90.

Bertrand D, Cooper E, Valera S, Rungger D, and Ballivet M (1991a) Electrophysiology of neuronal nicotinic acetylcholine receptors expressed in *Xenopus* oocytes following nuclear injection of genes or cDNA, in *Methods in Neuroscience* (Conn M, ed) pp 174–193, Academic Press, New York.

Bertrand D, Galzi JL, Devillers-Thiéry A, Bertrand S, and Changeux JP (1993) Mutations at two distinct sites within the channel domain M2 alter calcium permeability of neuronal *alpha* 7 nicotinic receptor. *Proc Natl Acad Sci USA* **90:**6971–6975.

Bertrand D, Valera S, Bertrand S, Ballivet M, and Rungger D (1991b) Steroids inhibit nicotinic acetylcholine receptors. *Neuroreport* **2:**277–280.

Bertrand S, Devillers-Thiéry A, Palma E, Buisson B, Edelstein SJ, Corringer PJ, Changeux JP, and Bertrand D (1997) Paradoxical allosteric effects of competitive

inhibitors on neuronal α7 nicotinic acetylcholine receptor. *Neuroreport* **8**:3591–3595.
Buisson B and Bertrand D (1998) Steroid modulation of the nicotinic acetylcholine receptor, in *Comparative Endocrinology* (Conn M, ed) Humana Press, Totowa, NJ.
Burg RW, Miller BM, Baker EE, Birnbaum J, Currie SA, Hartman R, Kong Y-L, Monaghan RL, Olson G, Putter I, Tunac JB, Wallick H, Stapley EO, Oiwa R, and Omura S (1979) Avermectins, new family of potent anthelmintic agents: producing organism and fermentation. *Antimicrob Agents Chemother* **15:**361–367.
Campbell WC (1989) *Ivermectin and Abamectin*. Springer-Verlag, New York.
Couturier S, Bertrand D, Matter JM, Hernandez MC, Bertrand S, Millar N, Valera S, Barkas T, and Ballivet M (1990) A neuronal nicotinic acetylcholine receptor subunit (*alpha* 7) is developmentally regulated and forms a homo-oligomeric channel blocked by *alpha*-BTX. *Neuron* **5:**847–56.
Cully DF, Vassilatis DK, Liu KK, Paress PS, Van der Ploeg LHT, Schaeffer JM, and Arena JP (1994) Cloning of an avermectin-sensitive glutamate-gated chloride channel from *Caenorhabditis elegans*. *Nature (Lond)* **371:**707–711.
Delbono O, Gopalakrishnan M, Renganathan M, Monteggia LM, Messi ML, and Sullivan JP (1997) Activation of the recombinant human *alpha*-7 nicotinic acetylcholine receptor significantly raises intracellular free calcium. *J Pharmacol Exp Ther* **280:**428–438.
Devillers-Thiéry A, Galzi JL, Bertrand S, Changeux JP, and Bertrand D (1992) Stratified organization of the nicotinic acetylcholine receptor channel. *Neuroreport* **3:**1001–1004.
Galzi JL, Bertrand S, Corringer PJ, Changeux JP, and Bertrand D (1996a) Identification of calcium binding sites that regulate potentiation of a neuronal nicotinic acetylcholine receptor. *EMBO J* **15:**5824–5832.
Galzi JL, Devillers-Thiéry A, Hussy N, Bertrand S, Changeux JP, and Bertrand D (1992) Mutations in the ion channel domain of a neuronal nicotinic receptor convert ion selectivity from cationic to anionic. *Nature (Lond)* **359:**500–505.
Galzi JL, Edelstein SJ, and Changeux JP (1996b) The multiple phenotypes of allosteric receptor mutants. *Proc Natl Acad Sci USA* **93:**1853–1858.
Gopalakrishnan M, Buisson B, Touma E, Giordano T, Campbell JE, Hu IC, Donnely-Roberts D, Arneric SP, Bertrand D, and Sullivan JP (1995) Stable expression and pharmacological properties of the human α7 nicotinic acetylcholine receptor. *Eur J Pharmacol Mol* **290:**237–246.
Gray R, Rajan AS, Radcliffe KA, Yakehiro M, and Dani JA (1996) Hippocampal synaptic transmission enhanced by low concentrations of nicotine. *Nature (Lond)* **383:**713–716.
Krusek J and Zemková H (1994) Effect of ivermectin on γ-aminobutyric acid-induced chloride currents in mouse hippocampal embryonic neurones. *Eur J Pharmacol* **259:**121–128.
Léna C and Changeux JP (1997) Role of Ca^{2+} ions in nicotinic facilitation of GABA release in mouse thalamus. *J Neurosci* **17:**576–585.
Lindstrom J (1996) Neuronal nicotinic acetylcholine receptors, in *Ion Channels*. (Narahashi T, ed) pp 377–450, Plenum Press, New York.
Mahmoud AAF (1995) Diseases due to helminths, in *Mandell, Douglas and Bennett's Principles and Practice of Infectious Diseases* (Mandell GL, Bennett JE, and Dolin R, eds) pp 2525–2537, Churchill Livingstone, New York.
Monod J, Wyman J, and Changeux JP (1965) On the nature of allosteric transitions: a plausible model. *J Mol Biol* **12:**88–118.
Mulle C, Léna C, and Changeux JP (1992) Potentiation of nicotinic receptor response by external calcium in rat central neurons. *Neuron* **8:**937–945.
Ottesen EA and Campbell WC (1994) Ivermectin in human medicine. *J Antimicrob Chemother* **34:**195–203.
Pacqué M, Muñoz B, Greene BM, and Taylor HR (1991) Community-based treatment of onchocerciasis with ivermectin: safety, efficacy, and acceptability of yearly treatment. *J Inf Dis* **163:**381–385.
Palma E, Bertrand S, Binzoni T, and Bertrand D (1996) Neuronal nicotinic α7 receptor expressed in *Xenopus* oocytes presents five putative binding sites for methyllycaconitine. *J Physiol (Lond)* **491:**151–161.
Peng X, Katz M, Gerzanich V, Anand R, and Lindstrom J (1994) Human α7 acetylcholine receptor: cloning of the α7 subunit from the SH-SY5Y cell line and determination of pharmacological properties of native receptors and functional α7 homomers expressed in *Xenopus* oocytes. *Mol Pharmacol* **45:**546–554.
Perutz MF, Fermi G, Abraham G, Poyart C, and Bursaux E (1986) Hemoglobin as a receptor of drugs and peptides: x-ray studies of the stereochemistry of binding. *J Am Chem Soc* **108:**1064–1078.
Puia G, Santi MR, Vicini S, Pritchett DB, Purdy RH, Paul SM, Seeburg PH, and Costa E (1990) Neurosteroids act on recombinant human $GABA_A$ receptors. *Neuron* **4:**759–765.
Rabow LE, Russek SJ, and Farb DH (1995) From ion currents to genomic analysis: recent advances in $GABA_A$ receptor research. *Synapse* **21:**189–274.
Revah F, Bertrand D, Galzi JL, Devillers-Thiéry A, Mulle C, Hussy N, Bertrand S, Ballivet M, and Changeux JP (1991) Mutations in the channel domain alter desensitization of a neuronal nicotinic receptor. *Nature (Lond)* **353:**846–849.
Rubin MM and Changeux JP (1966) On the nature of allosteric transitions: implications of nonexclusive ligand binding. *J Mol Biol* **21:**265–274.
Schönrock B and Bormann J (1993) Activation of Cl^- channels by avermectin in rat cultured hippocampal neurons. *Arch Pharm* **348:**628–632.
Sigel E and Baur R (1987) Effect of Avermectin B1a on chick neuronal γ-aminobutyrate receptor channels expressed in *Xenopus* oocytes. *Mol Pharmacol* **32:**749–752.
Valera S, Ballivet M, and Bertrand D (1992) Progesterone modulates a neuronal nicotinic acetylcholine receptor. *Proc Natl Acad Sci USA* **89:**9949–9953.
Warpman U and Nordberg A (1995) Epibatidine and ABT 418 reveal selective losses of *alpha*4 *beta*2 nicotinic receptors in Alzheimer brains. *Neuroreport* **6:**2419–2423.
Wevers A, Sullivan JP, Giordano T, Birtsch C, Monteggia LM, Nowacki S, Arneric S, and Schroder H (1995) Cellular distribution of the mRNA for the *alpha* 7 subunit of the nicotinic acetylcholine receptor in the human cerebral cortex. *Drug Dev Res* **36:**103–110.
Wonnacott S, Albuquerque EX, and Bertrand D (1993) Methyllycaconitine: a new probe that discriminates between nicotinic acetylcholine receptor subclasses, in *Receptors: Molecular Biology, Receptor Subclasses, Localization, and Ligand Design* (Conn PM, ed) pp 263–275, Academic Press, New York.

Send reprint requests to: D. Bertrand, Department of Physiology, University Medical Center, 1211 Geneva 4, Switzerland. E-mail: bertrand@cmu.unige.ch